Molecular Therapy
Oncolytics
Original Article

Combination of Detoxified Pneumolysin Derivative ΔA146Ply and Berbamine as a Treatment Approach for Breast Cancer

Hong Zhang,[1,2,5] Tao Zhu,[1,5] Ruoqiu Fu,[3] Yang Peng,[1] Peng Jing,[4] Wenchun Xu,[1] Hong Wang,[1] Sijie Li,[1] Zhaoche Shu,[1] Yibing Yin,[1] and Xuemei Zhang[1]

[1]Department of Laboratory Medicine, Key Laboratory of Diagnostic Medicine (Ministry of Education), Chongqing Medical University, Chongqing 400016, China; [2]Department of Laboratory Medicine, The Affiliated Hospital of North Sichuan Medical College and Department of Laboratory Medicine and Translational Medicine Research Center, North Sichuan Medical College, Nanchong 637000, China; [3]Department of Pharmacy, Daping Hospital, Army Medical University, Chongqing 400042, China; [4]Department of Pediatric Surgery, The Affiliated Hospital of North Sichuan Medical College, Nanchong 637000, China

Increasing evidence demonstrates that microorganisms and their products can modulate host responses to cancer therapies and contribute to tumor shrinkage via various mechanisms, including intracellular signaling pathways modulation and immunomodulation. Detoxified pneumolysin derivative ΔA146Ply is a pneumolysin mutant lacking hemolytic activity. To determine the antitumor activity of ΔA146Ply, the combination of ΔA146Ply and berbamine, a well-established antitumor agent, was used for breast cancer therapy, especially for triple-negative breast cancer. The efficacy of the combination therapy was evaluated *in vitro* using four breast cancer cell lines and *in vivo* using a synergistic mouse tumor model. We demonstrated that *in vitro*, the combination therapy significantly inhibited cancer cell proliferation, promoted cancer cell apoptosis, caused cancer cell-cycle arrest, and suppressed cancer cell migration and invasion. *In vivo*, the combination therapy significantly suppressed tumor growth and prolonged the median survival time of tumor-bearing mice partially through inhibiting tumor cell proliferation, promoting tumor cell apoptosis, and activating systemic antitumor immune responses. The safety analysis demonstrated that the combination therapy showed no obvious liver and kidney toxicity to tumor-bearing mice. Our study provides a new treatment option for breast cancer and lays the experimental basis for the development of ΔA146Ply as an antitumor agent.

INTRODUCTION

Breast cancer, one of the three most common cancers worldwide, is the most common malignancy in women.[1,2] Because of the changes of lifestyle and the initiation of screening programs, the morbidity of breast cancer is increasing over years. Many effective therapies, including endocrine therapy, neoadjuvant therapy, anti-human epidermal growth factor receptor 2 (HER2) targeting, and the combination, have been used in clinical practice, making substantial progress at breast cancer therapy. However, the mortality of breast cancer remains very high, being the most common cause of death from cancer in developing countries and second to lung cancer in developed countries.[1–3] What's worse, patients with breast cancer gradually became resistant to the existing therapies.[4,5] To achieve long-term disease control, there is an urgent need to discover and develop new, effective cancer drugs.[6]

Cancer immunotherapy has shown promising potential in the treatment of hematopoietic and solid tumors in recent years, achieving long-lasting complete responses and improving the overall survival in a fraction of patients with refractory or metastatic cancers.[7–14] In the context of cancer immunotherapy, immune checkpoint inhibitors have achieved unprecedented success both in preclinical models and in clinical practice, with increasing approved indications and an increased response rate. However, patients who benefited from checkpoint inhibitors are still limited.[15] An exciting discovery is that microorganisms can modulate host responses to cancer therapy, and several microorganisms and their products can directly contribute to tumor shrinkage.[16–24] However, the safety and specificity concerns impeded the development of live microorganisms as anticancer agents. Identification of specific components owing to the efficiency of live microorganisms may be the solution to the problem.[22,25]

Detoxified pneumolysin derivative ΔA146Ply is a pneumolysin mutant lacking hemolytic activity.[26] Our previous studies have proven that immunization with recombinant fusion protein ΔA146Ply-DnaJ protects mice from lethal *Streptococcus pneumoniae* infection,[27–29] whereas ΔA146Ply was used as an adjuvant. ΔA146Ply stimulation leads to increased secretion of interferon (IFN)-γ,

Received 4 March 2020; accepted 19 June 2020;
https://doi.org/10.1016/j.omto.2020.06.015.

[5]These authors contributed equally to this work.

Correspondence: Xuemei Zhang, Department of Laboratory Medicine, Key Laboratory of Diagnostic Medicine (Ministry of Education), Chongqing Medical University, 1 Yixueyuan Road, Yuzhong District, Chongqing 400016, People's Republic of China.
E-mail: zhangxuemei@cqmu.edu.cn

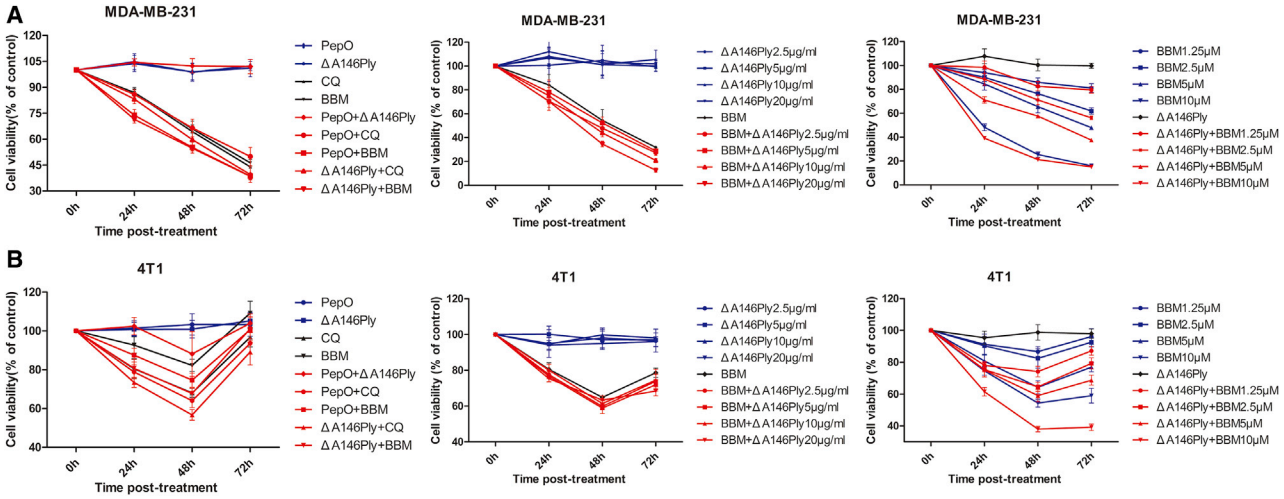

Figure 1. Cancer Cell Proliferation Inhibition by the Combination of ΔA146Ply and BBM

MDA-MB-231 cells (A) and 4T1 cells (B) were incubated with ΔA146Ply (10 μg/mL), PepO (10 μg/mL), BBM (5 μM), CQ (20 μM), or their combinations (left), with a range of ΔA146Ply concentrations (ΔA146Ply, 2.5–20 μg/mL) and a constant concentration of BBM (BBM, 5 μM; middle) or with a range of BBM concentrations (BBM, 1.25–10 μM) and a constant concentration of ΔA146Ply ΔA146Ply, 10 μg/mL; right) for the indicated time points. Proliferation was determined by CCK8 assays, and percentage viability was determined by comparing treatment conditions to medium control, which was normalized to 100. The data are shown as mean ± SD (n = 6).

interleukin (IL)-4, and IL-17A by splenocytes, indicating activation of helper T cell immune responses.[29] These results established the potential of ΔA146Ply as an immunomodulation agent. Increasing evidence has demonstrated that microorganisms and their products inhibit tumor growth, partially through intracellular signaling pathway modulation and immunomodulation.[18,22,23] Whether ΔA146Ply has anti-breast cancer activity or can enhance host responses to other antitumor therapies is still unknown.

Berbamine (BBM), isolated from traditional Chinese medicine (TCM) *Berberis amurensis*, is a natural bisbenzyl isoquinoline alkaloid.[30] It has long been used in clinical practice to treat patients with low levels of white blood cells caused by chemotherapy or radiotherapy.[30] It also protects the heart from ischemia/reperfusion injury in a preclinical model.[31] In addition, several studies have reported the antitumor activities of BBM against a variety of cancer types, including leukemia, liver cancer, lung cancer, and breast cancer.[32] In the context of breast cancer, BBM has been proven to inhibit tumor cell growth, migration, and invasion. Whether BBM suppresses breast cancer growth *in vivo* or enhances host responses to other antitumor therapies remains to be proven.

In the present study, we investigated the efficacy of the combination therapy of ΔA146Ply and BBM against breast cancer both *in vitro* and *in vivo*. We also evaluated the safety of the combination therapy *in vivo*. Our results demonstrated that the combination therapy significantly inhibited tumor cell proliferation, promoted cell apoptosis, caused cell-cycle arrest, and suppressed cell migration and invasion. *In vivo* the combination therapy significantly suppressed tumor growth and prolonged the median survival time of tumor-bearing mice. Mechanism studies showed that the combination therapy exerted antitumor activity partially through inhibiting tumor cell proliferation, promoting tumor cell apoptosis, and activating systemic antitumor immune responses *in vivo*. The safety analysis demonstrated that the combination therapy showed no obvious liver and kidney toxicity to tumor-bearing mice. Our study provides a new treatment option for breast cancer and lays the theoretical basis for the development of ΔA146Ply as an antitumor agent.

RESULTS

Cancer Cell Proliferation Inhibition by the Combination of ΔA146Ply and BBM

Previous research showed that chloroquine (CQ) has an anti-breast cancer effect.[33] In the present study, we used CQ and pneumoniae endopeptidase O (PepO) as an anti-breast cancer drug and protein controls, respectively. To determine the tumor-suppressive effect of ΔA146Ply, PepO, CQ, and BBM, breast cancer cell lines, including MDA-MB-231, PY8119, 4T1, and MCF-7, were cultured and incubated with ΔA146Ply, PepO, CQ, or BBM, either alone or in combination with each other for the indicated times. The cell viability was determined by the cell counting kit 8 (CCK8) assay. The data in Figures 1 and S1 show that ΔA146Ply or PepO alone exerted no or minimal tumor-suppressive effect on these four cell lines studied, and BBM or CQ alone inhibited their growth to a modest degree. The combination of ΔA146Ply or PepO and BBM or CQ significantly enhanced the tumor-suppressive effect of BBM or CQ, with a strongest inhibitory effect occurring at the combination of ΔA146Ply and BBM in MDA-MB-231 and MCF-7 cells. Therefore, we chose the combination of ΔA146Ply and BBM as a therapeutic option in the following studies.

Our results demonstrated that ΔA146Ply enhanced the tumor-suppressive effect of BBM in time- and dose-dependent manners on these

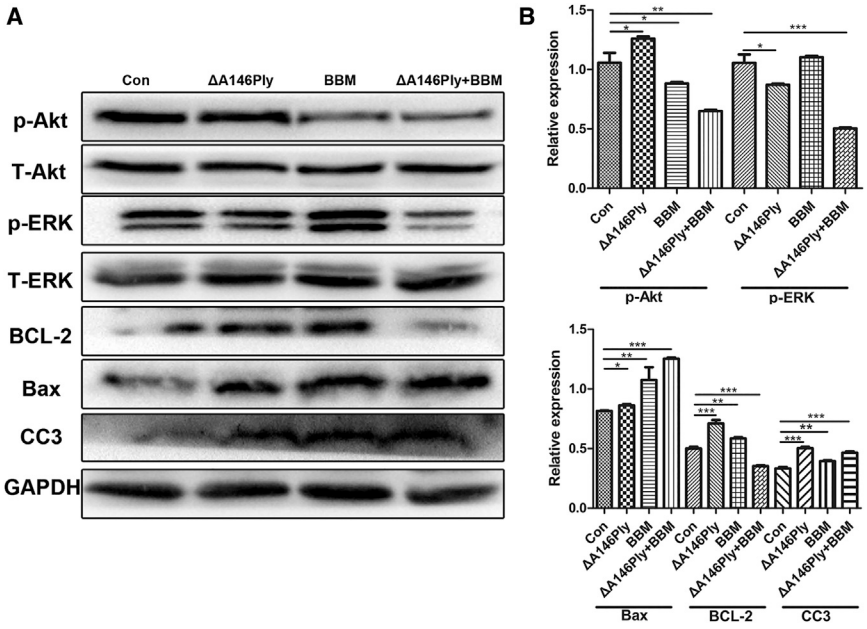

Figure 2. Intracellular Signaling Pathway Regulation by the Combination of ΔA146Ply and BBM

(A) MDA-MB-231 cells were incubated with ΔA146Ply (20 μg/mL), BBM (5 μM), or their combination for 48 h. Intracellular protein levels were determined by western blot (WB) analysis. Representative bands from three independent experiments with consistent results are shown. (B) Graphs show mean (±SD) protein levels normalized to total (T)-Akt (for p-Akt), T-ERK (for p-ERK), or GAPDH (for BCL-2, Bax, and CC3) (n = 3). Statistical analysis was performed by Student's t test. *p < 0.05, **p < 0.01, ***p < 0.001. CC3, cleaved caspase-3.

cells except 4T1. In 4T1 cells, the percentage viability at 72 h was higher than that at 48 h, indicating that the therapeutic effect cannot sustain 72 h, and maybe new drugs should be added after 48 h treatment to guarantee a better therapeutic effect. Also, the tumor-suppressive effects of different concentrations of BBM were enhanced by a constant concentration of ΔA146Ply.

Furthermore, we detected the levels of intracellular protein responsible for cell proliferation in MDA-MB-231 cells treated by ΔA146Ply, BBM, or their combination using western blot analysis. The data in Figure 2 show that the phosphorylation of Akt was slightly increased, whereas the phosphorylation of extracellular signal-regulated kinase (ERK) was decreased after ΔA146Ply treatment. BBM treatment modestly inhibited the phosphorylation of Akt. In the combination group, both phosphorylated (p)-Akt and p-ERK levels were significantly decreased compared with the control group, suggesting that the signaling proteins responsible for cell proliferation were inhibited by the combination therapy. Taken together, these results indicate that the combination of ΔA146Ply and BBM significantly inhibits breast cancer cell proliferation.

Cancer Cell Apoptosis Induction by the Combination of ΔA146Ply and BBM

To explore whether ΔA146Ply and BBM, either alone or in combination, can induce cancer cell apoptosis, these cells were cultured and treated with ΔA146Ply, BBM, or their combination at 37°C for 48 h. Cell apoptosis was analyzed by flow cytometry. The data in Figure 3A show that ΔA146Ply induced a modest apoptosis in MDA-MB-231 cells, whereas enhanced apoptosis was induced when combined with BBM. ΔA146Ply failed to induce the apoptosis of 4T1 cells, whereas BBM treatment increased the percentage of apoptotic 4T1 cells. Also, in the combination group, the percentage of apoptotic 4T1 cells was the highest (Figure 3B). Both ΔA146Ply and BBM induced the apoptosis of PY8119 cells, with the highest ratio of apoptotic cells in the combination group (Figure S2A). Figure S2B shows that ΔA146Ply modestly induced apoptosis of MCF-7 cells, whereas BBM failed to do so. The percentage of apoptotic MCF-7 cells did not differ between the combination group and the control group, suggesting that triple-negative breast cancer cell lines may be more susceptible to ΔA146Ply or BBM treatment in terms of apoptosis induction.

Furthermore, we detected the levels of intracellular protein responsible for cell apoptosis in MDA-MB-231 cells treated by ΔA146Ply, BBM, or their combination using western blot analysis. The data in Figure 2 show that the levels of cleaved caspase-3 (CC3) were increased in ΔA146Ply, BBM, and the combination group, as compared with the control group, indicating apoptosis introduction by ΔA146Ply, BBM, and their combination treatment. The levels of B-cell lymphoma 2 (BCL-2)-associated X protein (BAX), a proapoptotic protein, were also increased in ΔA146Ply, BBM, and the combination group compared with the control group, whereas the levels of BCL-2, an anti-apoptotic protein, were decreased significantly only in the combination group, which to some degree, explained the enhanced apoptosis induction effect by the combination therapy. Taken together, these results indicate that the combination of ΔA146Ply and BBM significantly induces apoptosis of triple-negative breast cancer cell lines with a synergistic effect compared with their single agent.

Cancer Cell-Cycle Arrest by the Combination of ΔA146Ply and BBM

To measure the difference of cell-cycle distribution after different treatment, cells were cultured and incubated with ΔA146Ply, BBM, or their combination at 37°C for 48 h. Cell-cycle distribution was analyzed by flow cytometry. The data in Figure 4A show that there was no significant difference in cell-cycle distribution among control, ΔA146Ply, and BBM groups in MDA-MB-231 cells. In the combination group, the ratio of G1-phase cells was increased, indicating that cell cycle was arrested at the G1 phase by the combination therapy.

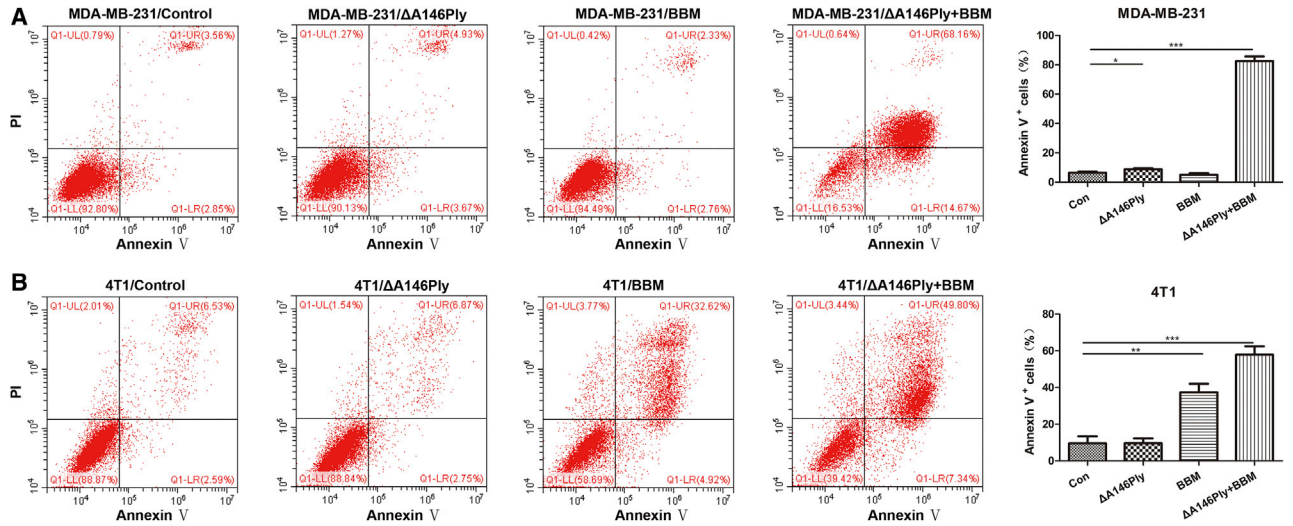

Figure 3. Cancer Cell Apoptosis Induction by the Combination of ΔA146Ply and BBM

MDA-MB-231 cells (A) and 4T1 cells (B) were incubated with ΔA146Ply (20 μg/mL), BBM (5 μM), or their combination for 48 h. Cell apoptosis was analyzed by flow cytometry. Representative pictures from one of three independent repeated experiments with consistent results are shown. Graphs show mean ± SD percentage of Annexin V^+ cells (n = 3). Statistical analysis was performed by Student's t test. *$p < 0.05$, **$p < 0.01$, ***$p < 0.001$.

Also, the distribution of cell cycle did not differ among control, ΔA146Ply, and BBM groups in 4T1 cells, whereas the ratio of S-phase cells was significantly increased in the combination group compared with the control group, indicating that cell cycle was arrested at the S phase by the combination therapy (Figure 4B). In PY8119 cells, the ratios of S-phase cells were increased in ΔA146Ply, BBM, and the combination group compared with the control group, indicating that cell cycle was arrested at the S phase by ΔA146Ply, BBM, and the combination therapy (Figure S3A). In MCF-7 cells, there was no significant difference in the distribution of cell cycle between the control and ΔA146Ply groups, whereas the ratios of G1-phase cells were increased in BBM and the combination groups compared with the control group, indicating that cell cycle was arrested at the G1 phase by BBM and the combination therapy (Figure S3B). Taken together, these results indicate that cell cycle is arrested at different phases in different cell lines by the combination therapy, with human breast cancer cell lines at the G1 phase and mouse breast cancer cell lines at the S phase.

Suppression of Cancer Cell Migration and Invasion by the Combination of ΔA146Ply and BBM

To determine the effect of ΔA146Ply, BBM, or their combination on the migration and invasion ability of cancer cells, high metastatic triple-negative breast cancer cell line MDA-MB-231 was used in this experiment. Cells were cultured and seeded on top of the Transwell inserts and incubated with ΔA146Ply, BBM, or their combination at 37°C for the indicated times. The migrated or invaded cells were stained with crystal violet and observed under a phase-contrast microscope. The data in Figure 5A show that ΔA146Ply significantly inhibited the migration of MDA-MB-231 cells, with a stronger effect than that of BBM. The migrated cells in the combination group were the least among these groups, suggesting that the combination therapy showed a synergistic suppression effect on the migration of MDA-MB-231 cells. The suppression effect of ΔA146Ply, BBM, or their combination on the invasion of MDA-MB-231 cells showed a similar tendency with the migration assay. The combination therapy also synergistically inhibited the invasion of MDA-MB-231 cells (Figure 5B). These results establish that the migration and invasion of MDA-MB-231 cells are significantly inhibited by the combination therapy.

Tumor Growth Suppression by the Combination of ΔA146Ply and BBM *In Vivo*

To determine the efficacy of the combination therapy *in vivo*, a syngeneic mouse tumor model was constructed by transplanting 4T1 cells to BALB/c mice. When tumor volumes reached 80–100 mm^3, the mice were randomly divided into four groups and intraperitoneally injected with normal saline, ΔA146Ply, or BBM, respectively. The treatment schedule is shown in Figure 6A. In brief, ΔA146Ply was injected every 4 days, and BBM was injected every other day. The data in Figure 6B show that the tumor volume was significantly smaller in the combination group than in the control group. Either ΔA146Ply or BBM treatment just mildly suppressed tumor growth. When used in combination, they showed a synergistic effect. There was no significant difference in the body weight among these four groups, which suggested that tumor-bearing mice tolerated ΔA146Ply or BBM treatment (Figure 6C). Although the combination therapy did not improve the overall survival of tumor-bearing mice, their median survival time was prolonged (Figure 6D). Figure 6E shows the picture of separated tumors at day 15 post-treatment, with the smallest tumor volumes in the combination group. Microscopically, heteromorphic nucleus cells were less, and the tumor cells became more ordered in

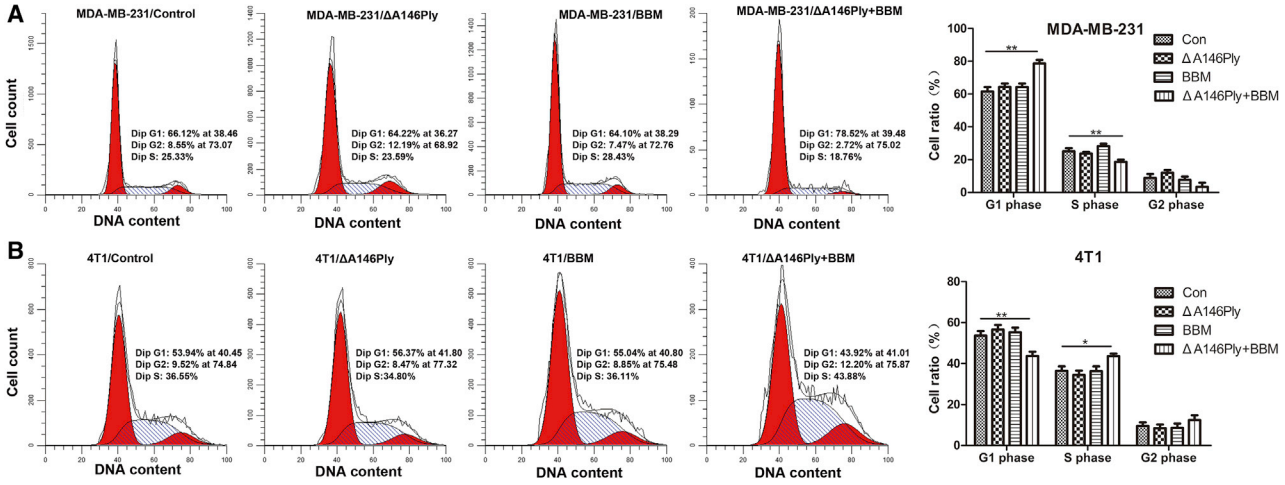

Figure 4. Cancer Cell-Cycle Arrest by the Combination of ΔA146Ply and BBM

MDA-MB-231 cells (A) and 4T1 cells (B) were incubated with ΔA146Ply (20 μg/mL), BBM (5 μM), or their combination for 48 h. Cell cycle was analyzed by flow cytometry. Representative pictures from one of three independent repeated experiments with consistent results are shown. Graphs show mean ± SD of cell ratios at different phases (n = 3). Statistical analysis was performed by Student's t test. *$p < 0.05$, **$p < 0.01$.

the combination group at days 9 and 15 after treatment, implying a response to the combination therapy (Figure 6F).

We further assessed the proliferation and apoptosis of tumor cells at days 9 and 15 after treatment among these groups using immunohistochemistry (IHC) analysis. As shown in Figure 7A, at the two time points, the levels of Ki67, a nucleoprotein responsible for cell proliferation, were significantly decreased in the combination group compared with the control group or their single-agent group, indicating a synergistic effect and a better response to the combination therapy. Furthermore, the levels of CC3, a protein responsible for cell apoptosis, were significantly increased in the combination group compared with the control group or their single-agent group at these time points (Figure 7B). The method of terminal deoxynucleotidyl transferase (TdT)-mediated deoxyuridine triphosphate (dUTP) nick end labeling (TUNEL) was also used to detect apoptosis of tumor cells. The data in Figure 7C show that the ratio of apoptotic cells was significantly increased in the combination group compared with the control group or their single-agent group both at day 9 and at day 15 post-treatment. Taken together, these results establish that the combination therapy significantly suppresses tumor growth *in vivo* partially through inhibiting tumor cell proliferation and promoting tumor cell apoptosis.

Activation of Systemic Antitumor Immunity by the Combination of ΔA146Ply and BBM *In Vivo*

Increasing evidence has demonstrated that microorganisms and their products can inhibit tumor growth via activating systemic antitumor immunity.[22,23] ΔA146Ply has been shown to induce apoptosis of cancer cells via modulating an intracellular signaling pathway by our above results. Whether it activates host antitumor immune responses remains to be determined. To answer this question, tumor-bearing mice treated with ΔA146Ply, BBM, or their combination were sacrificed, and their tumor tissues and serum were collected for cytokines and tumor-infiltrating myeloid and lymphoid subsets analysis. The data in Figure 8 show that the concentrations of cytokines measured in tumor tissues did not differ among these groups, either at day 9 or at day 15 post-treatment. Although there was no significant difference in the concentrations of cytokines measured in serum at day 9 post-treatment, the concentrations of IL-10 and IL-4 in the combination therapy group showed a decreased tendency compared with the control group. At day 15 post-treatment, the concentrations of IFN-γ in serum were significantly increased in BBM and the combination groups compared with the control group, with a higher concentration of IFN-γ in the combination group. Moreover, at this time point, the concentrations of IL-4 and IL-10 in serum of the combination group showed a decreased tendency compared with the control group. These results indicate the activation of systemic antitumor immune responses.

We further analyzed tumor-infiltrating myeloid and lymphoid subsets by flow cytometry. The data in Figure 9 show that the ratio of macrophages and dendritic cells did not differ among these groups both at day 9 and at day 15 post-therapy. In terms of tumor-infiltrating lymphoid subsets, we found that the ratio of $CD8^+$ T cells was significantly increased in the ΔA146Ply group compared with the control group, both at day 9 and at day 15 post-treatment. Unexpectedly, the ratio of $CD4^-CD8^-$ T cells in the combination therapy was significantly increased compared with the control group, both at day 9 and at day 15 post-treatment, suggesting an antitumor role played by $CD4^-CD8^-$ T cells in the combination therapy. Moreover, the ratio of regulatory T (Treg) cells was significantly decreased in ΔA146Ply, BBM, and the combination group compared with the control group, with a more obvious decrease occurring in the combination group. Taken together, these results suggest that the combination therapy suppresses tumor growth *in vivo* partially through increasing

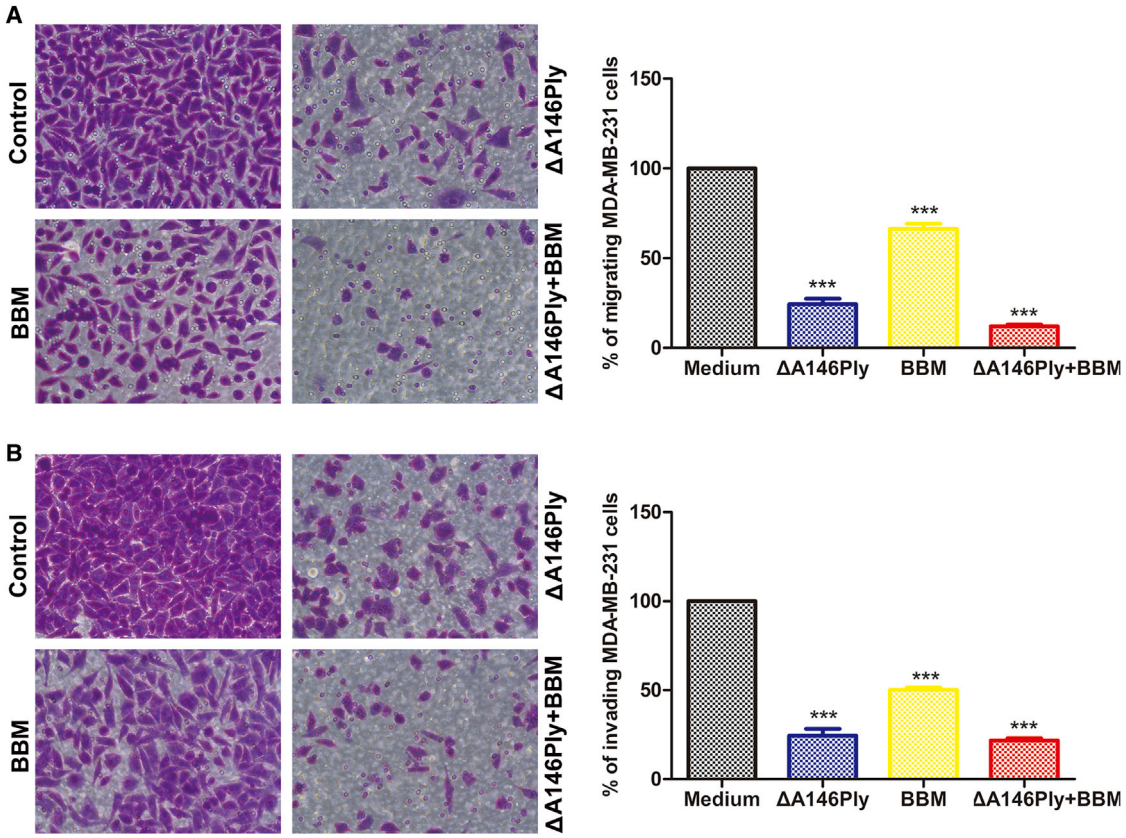

Figure 5. Suppression of Cancer Cell Migration and Invasion by the Combination of ΔA146Ply and BBM

(A) MDA-MB-231 cells were incubated with ΔA146Ply (20 μg/mL), BBM (5 μM), or their combination for 18 h. Representative images (original magnification, ×20) of these cells migrating through Transwell inserts toward serum are shown. Graph shows the average (±SD) percentage of migrating cells normalized to medium control (with control set as 100%) (n = 3). (B) MDA-MB-231 cells were incubated with ΔA146Ply (20 μg/mL), BBM (5 μM), or their combination for 24 h. Representative images (original magnification, ×20) of these cells invading through Transwell inserts toward serum are shown. Graph shows the average (±SD) percentage of invading cells normalized to medium control (with control set as 100%) (n = 3). Statistical analysis was performed by Student's t test. ***$p < 0.001$.

the ratio of $CD4^{-}CD8^{-}$ T cells and decreasing the ratio of Treg cells in tumor-infiltrating lymphoid subsets.

Safety Analysis of the Combination Therapy *In Vivo*

To determine the safety of the combination therapy *in vivo*, tumor-bearing mice treated by ΔA146Ply, BBM, or their combination were sacrificed, and their blood, lungs, livers, and kidneys were collected for biochemical and pathologic analysis. The data in Figure 10A show that alanine transaminase (ALT), aspartate transaminase (AST), and urea levels did not differ between the healthy control group and tumor groups at day 9 post-therapy. At day 15 post-therapy, AST levels were significantly increased in tumor groups compared with the healthy control group, but there was no significant difference among tumor groups, indicating that the increase of AST was caused by tumor instead of tumor therapy. At that time point, both ALT and urea levels did not differ between the healthy control group and tumor groups. What's more, there was no obvious damage in liver and kidney tissues after 9 and 15 days of treatment, according to the gross specimens and pathological sections (Figures 10B–10D). From the gross specimens of lung tissues, we observed that lung injury was alleviated by ΔA146Ply, BBM, and the combination therapy at days 9 and 15 post-treatment (Figure 10B). The pathological sections also showed alleviation of lung injury in ΔA146Ply and the combination groups, with less broken alveoli and thinner alveolar walls (Figures 10C and 10D). At day15 post-treatment, metastasis lesions were observed in the lungs of the control group, not in the treatment groups, suggesting that ΔA146Ply, BBM, and the combination therapy effectively inhibit tumor metastasis (Figure 10D). Taken together, these results suggest that the combination therapy showed no obvious liver and kidney toxicity to tumor-bearing mice, alleviated lung injuries of tumor-bearing mice, and effectively inhibited tumor metastasis.

DISCUSSION

In this study, we provide evidence that the combination of ΔA146Ply and BBM significantly inhibited cell proliferation, promoted cell apoptosis, caused cell-cycle arrest, and suppressed cell migration and invasion of breast cancer cell lines, and *in vivo*, the combination therapy significantly suppressed tumor growth and prolonged the

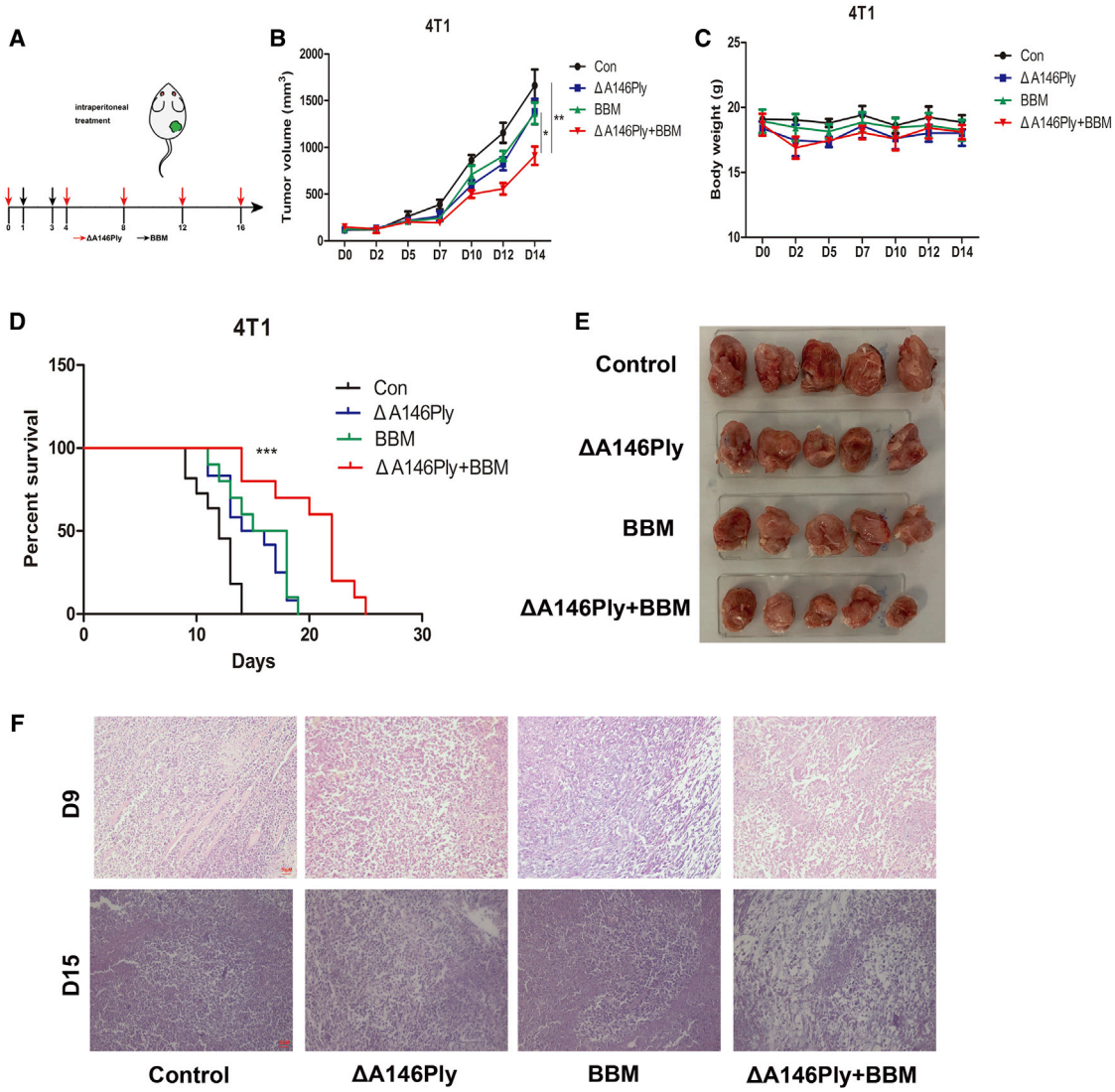

Figure 6. Tumor Growth Suppression by the Combination of ΔA146Ply and BBM *In Vivo*

(A) Treatment schedule. BALB/c mice (n = 5 mice per group) were subcutaneously implanted with 1×10^6 4T1 cells in the right hind flank. When tumor volumes reached 80–100 mm^3, mice received intraperitoneal injections of ΔA146Ply (200 μg) every 4 days and BBM (50 mg/kg) every other day. (B) Tumor growth curves of untreated and treated tumors (*$p < 0.05$, **$p < 0.01$, two-way ANOVA with Tukey's multiple comparisons test). Data are representative of two independent repeated experiments. (C) Body weights of untreated and treated mice. (D) Kaplan-Meier survival curves for 4T1-bearing mice (n = 10 per group, ***$p < 0.001$, log-rank [Mantel-Cox test]). (E) Representative pictures of separated tumors from ΔA146Ply, BBM, or their combination of treated mice at the end of the experiment. (F) Representative images (original magnification, ×20) of tumor sections stained with hematoxylin-eosin at day 9 and day 15 post-treatment.

median survival time of tumor-bearing mice. Furthermore, using a syngeneic mouse tumor model, we demonstrated that the combination therapy exerted antitumor activity partially through inhibiting tumor cell proliferation, promoting tumor cell apoptosis, and activating systemic antitumor immune responses. Safety analysis showed that there was no obvious liver and kidney toxicity with the combination therapy.

Triple-negative breast cancer is the most malignant and intractable breast cancer with limited treatment options.[34] Our study provides a novel treatment option for triple-negative breast cancer. The combination of ΔA146Ply and BBM showed a synergistic therapeutic effect against triple-negative breast cancer. The anti-breast cancer effect of BBM has long been established.[32] Our study proved for the first time that a mutant of pneumococcal virulence protein combined with BBM contributes to better tumor control. Microorganisms used for tumor therapy have long been established by William B. Coley, who recognized the anticancer effect of bacteria against sarcoma since 1876.[35] Since then, an increasing number of microorganisms and their products were proven to show antitumor activity against

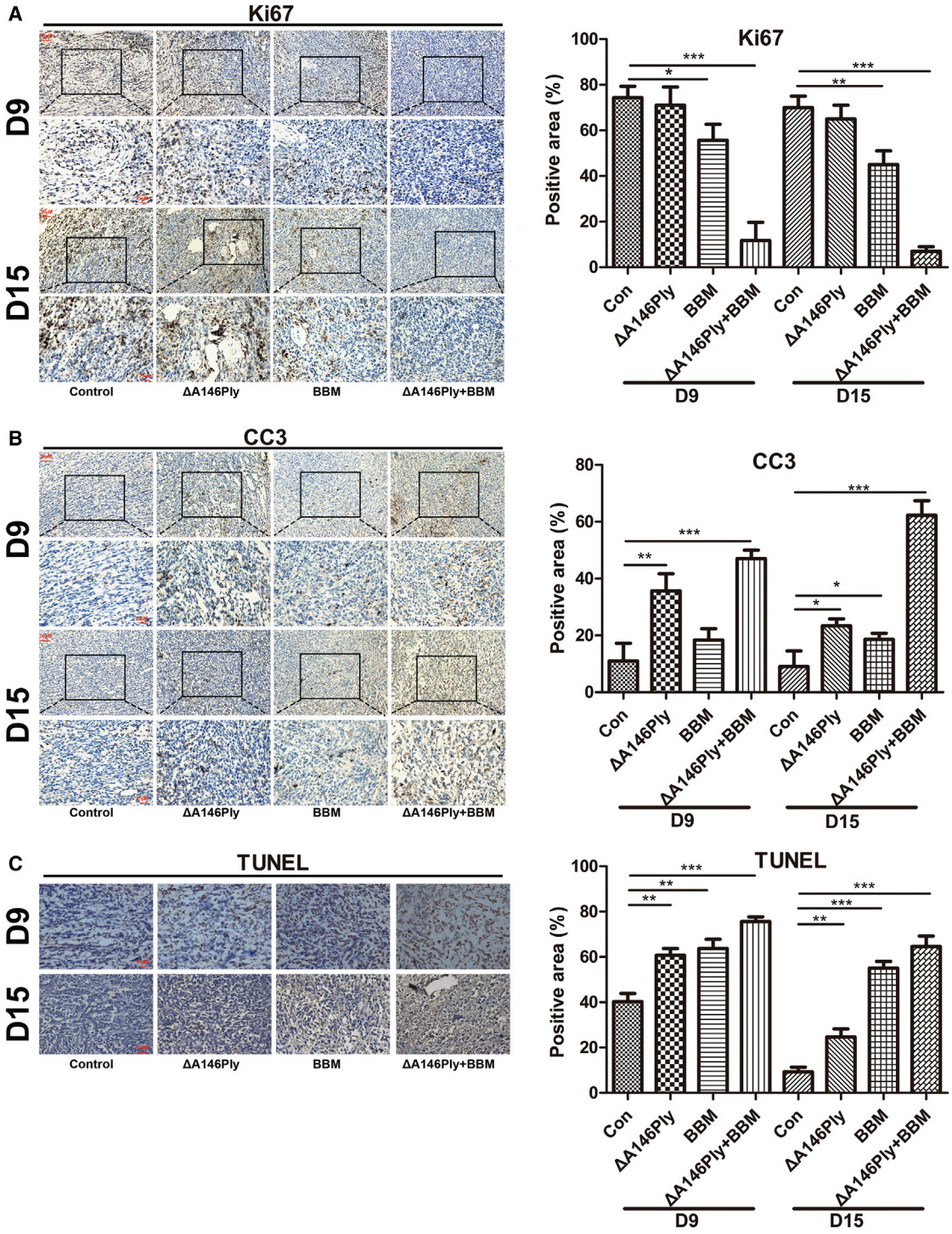

Figure 7. The Proliferation Inhibition and Apoptosis Induction by the Combination of ΔA146Ply and BBM *In Vivo*

(A and B) Immunohistochemistry (IHC) analysis was performed using the proliferation marker Ki67 (A) and the apoptosis marker CC3 (B) to determine the proliferation and apoptosis of tumor sections at days 9 and 15 post-treatment. (C) TUNEL assay was also performed to determine the apoptosis of tumor sections. Representative images (original magnification, ×40) and quantification are shown from two independent repeated experiments. Graphs show mean (±SD) percentage of positive area (n = 3). Statistical analysis was performed by Student's t test. *$p < 0.05$, **$p < 0.01$, ***$p < 0.001$. CC3, cleaved caspase-3.

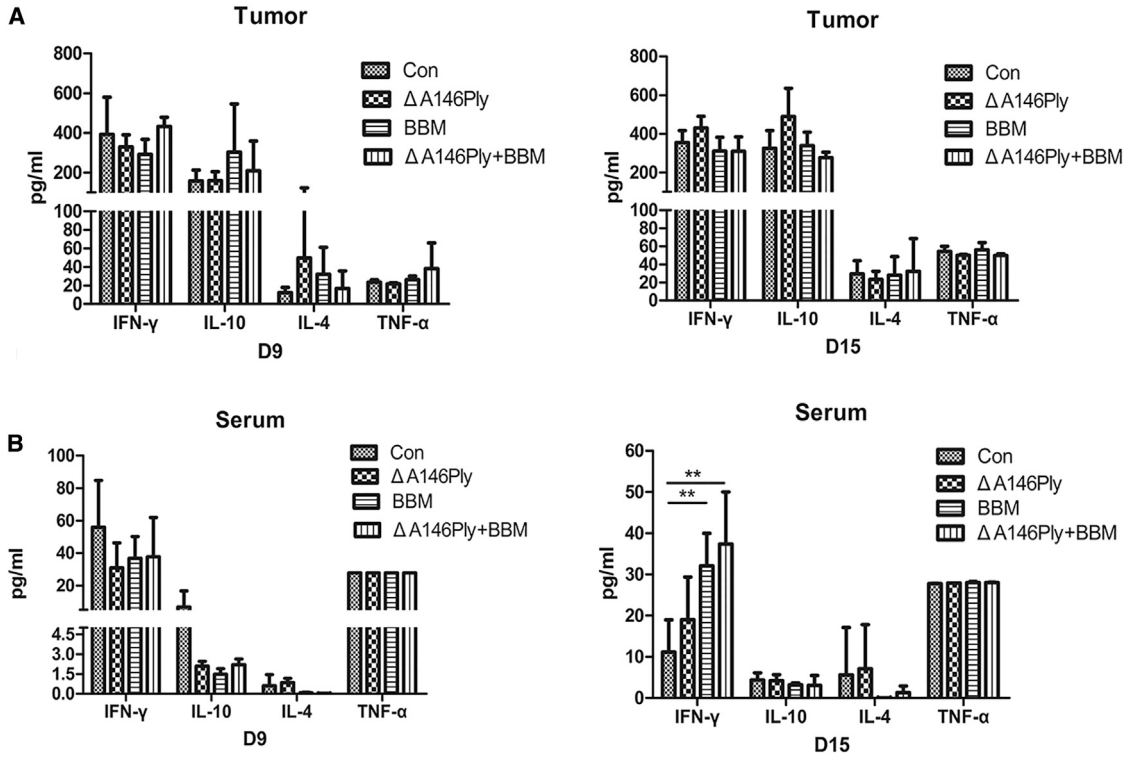

Figure 8. The Concentrations of Cytokines in Tumor Tissues and Serum

(A and B) ELISA assays were performed to determine IFN-γ, IL-10, IL-4, and TNF-α levels in tumor tissues (A) and serum (B) at days 9 and 15 post-treatment. The data are shown as mean (±SD) protein levels of at least 3 mice per group. Statistical analysis was performed by Student's t test. *$p < 0.05$, **$p < 0.01$, ***$p < 0.001$.

various tumors or modulate host responses to other therapies.[18,22,23] However, substantial progress has not been made in the field of cancer microorganism therapy. Only few microorganisms have been used in clinical practice to treat cancer, with examples of an attenuated form of *Mycobacterium bovis* for superficial bladder cancer treatment and oncolytic herpes virus for melanoma treatment.[36,37] A main reason for this situation may be the safety concerns for live microorganisms as antitumor agents.[18,22] Our study provides new evidence of a bacterial product, especially a pathogen's product used for cancer treatment. A certain product would avoid the safety concerns of live microorganisms and contribute to tumor control.

In the present study, ΔA146Ply treatment alone did not inhibit cancer cell proliferation, but it induced significant apoptosis of cancer cells, which may explain the enhanced inhibitory effect of the combination therapy on cell proliferation. The effect of ΔA146Ply on proliferation and apoptosis of breast cancer cells seems to contradict each other. A possible reason for this contradiction may be that ΔA146Ply treatment simultaneously promotes cancer cell proliferation and apoptosis, resulting in not a decreased cell number. The combination therapy significantly inhibited proliferation of MCF-7 cells, but it did not induce apoptosis of these cells, indicating that proliferation inhibition and apoptosis induction are two independent cellular processes. Therapies targeting proliferation and apoptosis simultaneously may contribute to better tumor control.[38–40] This assumption is also supported by the study of Rahmani et al.,[41] where they proved cotargeting BCL-2 and phosphatidylinositol 3-kinase (PI3K) used for acute myelogenous leukemia (AML) treatment.

In the context of migration and invasion inhibition by ΔA146Ply treatment in MDA-MB-231 cells, our results indicate that ΔA146Ply has the potential to inhibit metastasis of triple-negative breast cancer. Increasing evidence has demonstrated that inflammasome activation promotes metastasis of breast cancer.[42–45] Littmann et al.[46] proved that wild-type pneumolysin inhibited inflammasome activation of human dendritic cells, suggesting that ΔA146Ply may inhibit metastasis of breast cancer through suppressing activation of inflammasome. Whether inflammasome plays a role in our current system remains to be determined. To understand this process in detail, further research is still needed.

In vivo, the combination therapy suppressed tumor growth partially through inhibiting tumor cell proliferation and promoting tumor cell apoptosis, which is consistent with our findings *in vitro*. Furthermore, systemic antitumor immune responses were activated by the combination therapy *in vivo*, with evidence of elevated IFN-γ levels in serum of tumor-bearing mice (Figure 8B). This effect also contributes to tumor growth suppression. The immunomodulation effect of

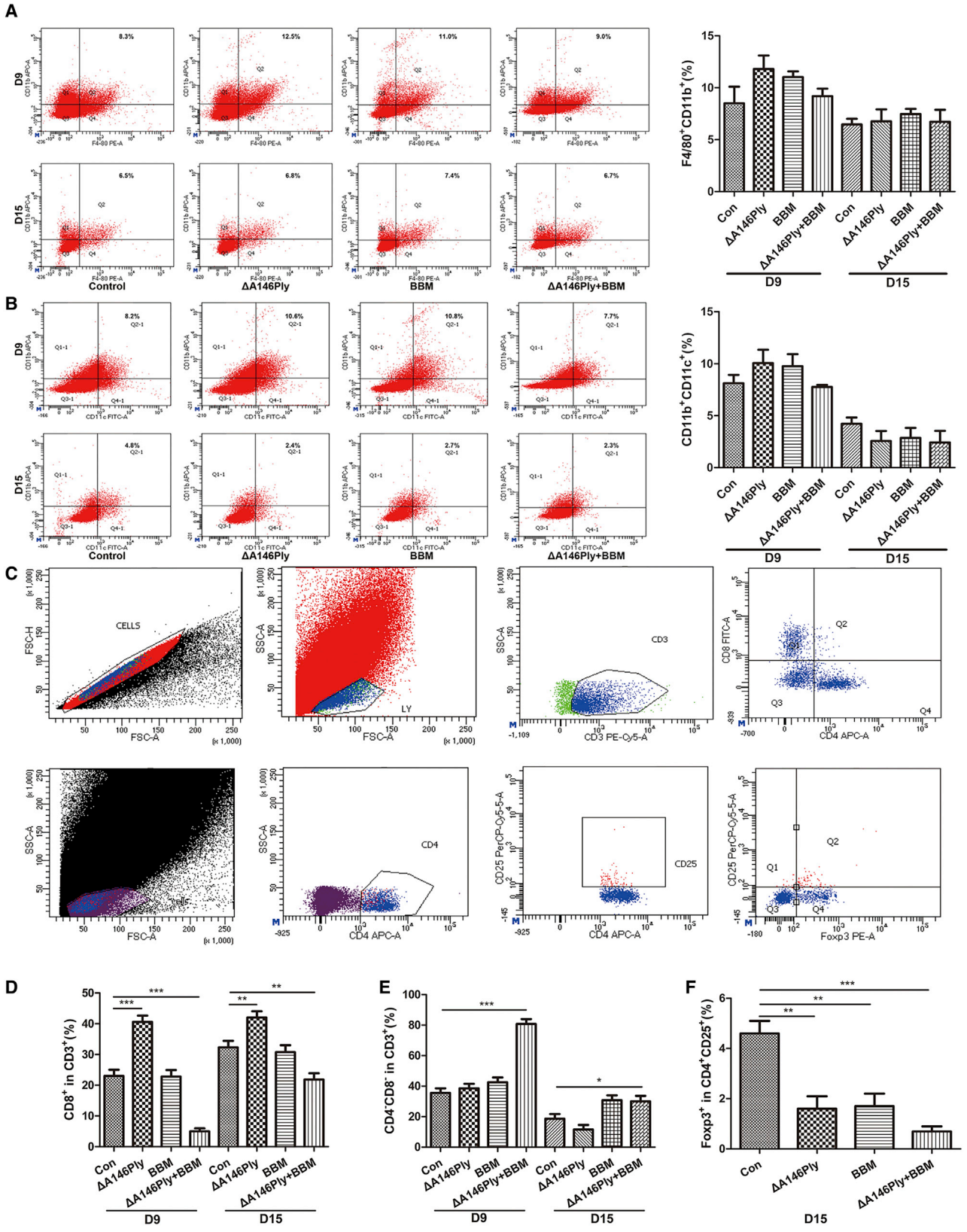

(legend on next page)

ΔA146Ply has long been proven by our previous studies.[27–29] In the current system, the activation of systemic antitumor immune responses may not be merely mediated by ΔA146Ply, because at day 15 post-treatment, serum IFN-γ levels were significantly increased in the BBM group compared with the control group, indicating activation of a systemic immune response by BBM treatment. These findings indicate for the first time, at least to our knowledge, that BBM may also exert an immunomodulation effect on tumor-bearing mice. As previous studies on the antitumor effect of BBM have always concentrated on intracellular signaling pathway modulation by BBM treatment,[32,47,48] little attention has been given to its immunomodulation effect. A possible reason for this situation may be that a previous mouse model was constructed using a nude mouse, in which its cellular immunity is deficient.[49–51] However, the detailed mechanisms by which BBM or the combination therapy activates systemic antitumor immune responses remain to be determined.

In vivo, ΔA146Ply treatment alone enhanced the ratio of $CD8^+$ T cells in tumor-infiltrating lymphocytes both at day 9 and at day 15 post-treatment, which may contribute to tumor growth suppression. In the combination therapy group, the ratio of $CD8^+$ T cells in tumor-infiltrating lymphocytes did not increase; instead, the ratio of $CD4^-CD8^-$ T cells significantly increased, indicating that other lymphocytes play a role in this system. A variety of research has proven that γδ T cells play an important role in antitumor immune responses.[52–57] γδ T cells are $CD4^-CD8^-$ T cells;[58] therefore, we could speculate that the increased $CD4^-CD8^-$ T cells in the combination group were γδ T cells. To support our hypothesis, further research is still needed. Their functions and regulation mechanisms in our current system remain to be investigated by our following studies.

Although our results demonstrated that the combination of ΔA146Ply and BBM synergistically suppressed tumor growth *in vivo*, it seems that ΔA146Ply and BBM may exert different roles in host immunomodulation, with evidence of differences in serum IFN-γ levels and tumor-infiltrating lymphocytes subsets between ΔA146Ply and BBM group (Figures 8 and 9). Therefore, deeper insight into the immunomodulation mechanisms of ΔA146Ply and BBM would provide a theoretical basis for the rational design of their combination in cancer immunotherapy. Our study provides a treatment option of the combination of ΔA146Ply, a pathogen's product, and BBM, a monomer of TCM for breast cancer. The combination of ΔA146Ply or BBM and other therapies, including chemotherapy, radiotherapy, and immunotherapy, may achieve a better therapeutic effect.

Taken together, in the present study, we determined the efficacy and safety of the combination therapy of ΔA146Ply and BBM, providing a novel therapeutic option for breast cancer, especially for triple-negative breast cancer. In the future, we will further investigate the mechanisms by which ΔA146Ply exerts antitumor activities, laying the experimental basis for the rational design of the combinations with ΔA146Ply.

MATERIALS AND METHODS

Mice

Specific pathogen-free, 5- to 6-week-old female BALB/c mice were purchased from Beijing HFK Bioscience (Beijing, China) and maintained at Chongqing Medical University. All mice were maintained with sterile water and mouse chow *ad libitum* under barrier conditions. All experimental procedures were approved by the Ethics Committee of Chongqing Medical University.

Cell Lines

Human triple-negative breast cancer cell line MDA-MB-231, mouse triple-negative breast cancer cell lines 4T1 and PY8119, and human estrogen receptor-α-positive breast cancer cell line MCF-7 were purchased from the American Type Culture Collection (ATCC) and cultured according to their constructions to a rough confluency of 75%. Briefly, these cells, except 4T1, were cultured with Dulbecco's modified Eagle's medium (DMEM) (HyClone, Barrington, IL, USA), supplemented with 10% fetal bovine serum (FBS) (Biological Industries, Kibbutz Beit Haemek, Israel) and 1% penicillin-streptomycin (HyClone, Barrington, IL, USA) in 5% CO_2 at 37°C. 4T1 cells were cultured with RPMI-1640 medium (Gibco), supplemented with 10% FBS and 1% penicillin-streptomycin.

Preparation of ΔA146Ply and *Streptococcus* PepO Protein

PepO is a ubiquitously expressed pneumococcal virulence protein and used as protein control in the present study[59]. The preparation of ΔA146Ply and PepO protein has been described in detail previously.[27,59] The Ni^{2+}-charged column chromatograph used for protein purification was purchased from GE Healthcare (Buckinghamshire, UK). Polymyxin B agarose used for lipopolysaccharide (LPS) removal was purchased from GenScript (New Jersey, USA). These protein preparations contained no detectable LPS when they were detected by the Limulus amebocyte lysate assay, and the concentrations of the protein preparation were determined by the bicinchoninic acid (BCA) assay.

CCK8 Assay

3,000 cells were seeded in 96-well plates and cultured for 24 h before the addition of the protein or drug. These cells were then incubated with ΔA146Ply, PepO, BBM (Sigma-Aldrich, St. Louis, MO, USA), and CQ, either alone or in combination with each other, at different

Figure 9. Flow Cytometry Analysis of Tumor-Infiltrating Myeloid and Lymphoid Subsets

(A and B) Flow cytometry analysis was performed using the myeloid marker CD11b, the mature macrophage marker F4/80 (A), and the dendritic cell marker CD11c (B) to determine the tumor-infiltrating myeloid subsets at day 9 and day 15 post-treatment. Representative images from one of two independent experiments are shown. Graphs show mean (±SD) percentage of macrophages or dendritic cells (n = 3). (C) The gating strategies for tumor-infiltrating CD4- or CD8-positive T cells (top) and tumor-infiltrating Treg cells (bottom). (D–F) The percentages of tumor-infiltrating $CD8^+$ T cells (D), $CD4^-CD8^-$ T cells (E), and Treg cells (F) of tumor-bearing mice at days 9 and 15 post-treatment. The data are shown as mean ± SD (n = 3). Statistical analysis was performed by Student's t test. *$p < 0.05$, **$p < 0.01$, ***$p < 0.001$.

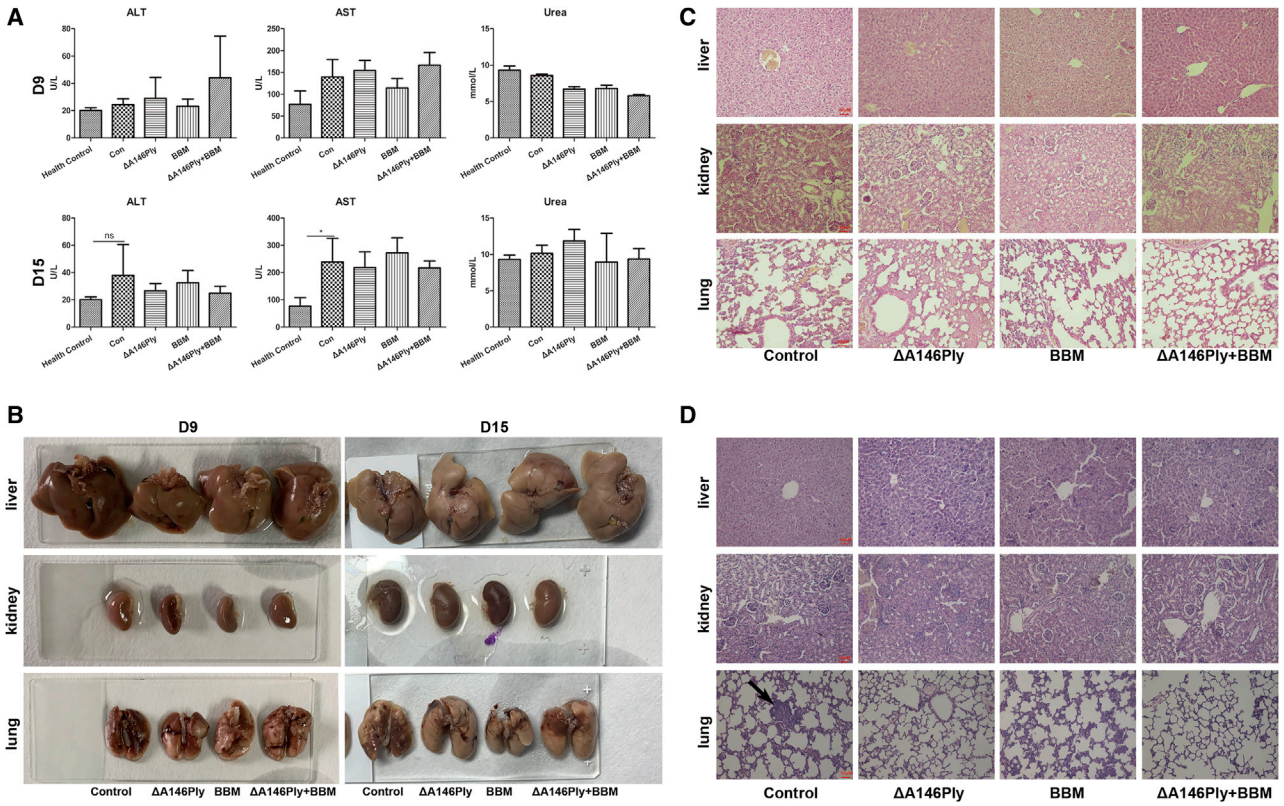

Figure 10. Safety Analysis of the Combination Therapy *In Vivo*

(A) Biochemical analysis was performed to determine ALT, AST, and urea levels in serum of tumor-bearing mice at days 9 and 15 post-treatment. The data are shown as mean (±SD) levels of at least 3 mice per group (Student's t test). *$p < 0.05$; ns, not significant. (B) Representative images of livers, kidneys, and lungs from tumor-bearing mice at days 9 and 15 post-treatment. (C and D) Representative images (original magnification, ×20) of liver, kidney, and lung sections from tumor-bearing mice at day 9 (C) and at day 15 (D) post-treatment. The black arrow indicates a metastatic lesion.

concentrations for indicated times (24 h, 48 h, and 72 h). Proliferation was determined with the use of the CCK8 reagent, according to the manufacturer's directions. 2 h later, the absorbance at 450 nm was quantified. The percentage viability was determined by normalizing the treated values to control (medium-treated) samples.

Flow Cytometry Analysis

For apoptosis and cell-cycle analysis, 1×10^5 cells were seeded in 6-well plates and cultured for 24 h before addition of the protein or drug. These cells were then incubated with ΔA146Ply (20 μg/mL) or BBM (5 μM), either alone or in combination, for 48 h. Subsequently, the cells were collected and washed twice with prechilled phosphate buffer solution (PBS). For apoptosis analysis, the cells were stained with fluorescein isothiocyanate (FITC)-labeled Annexin V and phosphatidylinositol (PI) in the dark for 30 min, followed by twice washing and resuspension with PBS for detection. For cell-cycle analysis, cells were fixed with prechilled 75% alcohol at 4°C overnight and stained with PI in the dark for 30 min.

For tumor-infiltrating myeloid and lymphoid subset analysis, tumor tissues were collected on day 9 and day 15 after the initiation of therapy. Subsequently, tumors were cut into about 1 mm^3 pieces and digested with collagenase IV (1 mg/mL; Sigma-Aldrich) in DMEM at 37°C for 30 min to collect single-cell populations. After termination of digestion with an equal volume of DMEM, supplemented with 10% FBS, cells were filtrated through 75 μm cell strainers; treated with red blood cell lysis buffer (Sangon, Shanghai, China); washed in PBS; and stained with extracellular antibodies, including anti-CD11b (Becton Dickinson [BD]), anti-CD11c (eBioscience), anti-F4/80 (BD), anti-CD3 (BD), anti-CD4 (eBioscience), anti-CD8 (eBioscience), and anti-CD25 (BioLegend). For FOXP3 staining, cells were fixed and permeabilized with the FOXP3/transcription factor staining buffer, according to the manufacturer's instructions. Anti-FOXP3 antibody (Invitrogen) was used for intracellular staining. All samples were analyzed with the use of a BD LSRFortessa cell analyzer.

Transwell Assay

Boyden chambers using filters (8 μm pore size; Corning Costar) were used for migration and invasion assays. The filters were coated with Matrigel (BD) before use for invasion assays. Briefly, 5×10^4 MDA-MB-231 cells were seeded on top of the insert and incubated with ΔA146Ply (20 μg/mL) or BBM (5 μM), either alone or in

combination, at 37°C for 18 h (migration assay) or 24 h (invasion assay). DMEM, supplemented with 20% FBS, was added to the lower chamber. After fixation with 4% paraformaldehyde, the filters were stained with 0.1% crystal violet in PBS for 20 min. Nonmigrated cells in the upper side of the filters were scrapped off, and the filters were observed under a phase-contrast microscope.

Western Blot Analysis

1×10^6 MDA-MB-231 cells were seeded in 6 cm dishes and cultured for 24 h before addition of the protein or drug. Then, the cells were treated with ΔA146Ply (20 μg/mL) or BBM (5 μM), either alone or in combination, at 37°C for 48 h. After washing with prechilled PBS, the cells were collected and lysed with radioimmunoprecipitation assay (RIPA; BiYunTian, Shanghai, China) containing a phosphorylase inhibitor and protease inhibitor (Bimake). After the protein concentrations were determined, SDS loading buffer was added to the samples. Then, these samples were boiled for 10 min and centrifuged at 12,000 × *g* for 10 min to remove cell debris. An equal volume of protein was separated using SDS-PAGE gel and transferred to a polyvinylidene fluoride (PVDF) membrane (Millipore, Bedford, MA). After blocking with 5% de-fatted milk at 37°C for 2 h, the membrane was probed with the indicated monoclonal antibody at 4°C overnight. These monoclonal antibodies included anti-phospho-Akt (Cell Signaling Technology), anti-total-Akt (Cell Signaling Technology), anti-phospho-ERK (Cell Signaling Technology), anti-total-ERK (Cell Signaling Technology), anti-CC3 (Cell Signaling Technology), anti-BCL-2 (Santa Cruz Biotechnology), anti-Bax (Santa Cruz Biotechnology), and anti-glyceraldehyde 3-phosphate dehydrogenase (GAPDH; Cell Signaling Technology). After washing for 4 times, the membrane was incubated with corresponding horseradish peroxidase-labeled secondary goat anti-mouse or goat anti-rabbit antibodies at 37°C for 1 h, followed by 4 washing procedures. The antigen-antibody complexes were detected using a Bio-Rad chemiluminescence detection system, and the expression of GAPDH was used as endogenous reference.

Subcutaneous Tumor Model in Mice

Mice were subcutaneously inoculated in the right hind flank with 1×10^6 4T1 cells in 0.1 mL PBS per mouse. Vernier calipers were used to measure across two diameters of the tumor, and the formula: volume (V) = length × width^2 × 0.5 was used to calculate the tumor volume. 7 days after the inoculation, when tumors reached 80–100 mm^3, mice were randomly divided into four groups (five mice per group for tumor volume analysis and ten mice per group for survival analysis) and intraperitoneally injected with 0.2 mL normal saline for the control group, 200 μg ΔA146Ply in 0.2 mL normal saline for the ΔA146Ply group and the combination group, and 50 mg/kg BBM in 0.2 mL normal saline for the BBM group and the combination group. ΔA146Ply was injected every 4 days, and BBM was injected every other day. The tumor size and body weight were measured every other day. Mice were euthanized when the tumors reached a volume of ~1,500 mm^3.

Hematoxylin and Eosin Staining

Whole tumors, lungs, livers, and kidneys from euthanized BALB/c mice were fixed with 4% paraformaldehyde, dehydrated with ethanol series, embedded in paraffin, and sectioned into 5 μm series sections. These sections were then stained with hematoxylin-eosin and observed under a light microscope.

IHC

The tumor sections were de-waxed with xylene, hydrated with ethanol series, treated with sodium citrate at 95°C for 15 min for antigen retrieval, and incubated in 3% H_2O_2 to inhibit endogenous peroxidase. After blocking nonspecific staining with PBS containing 1% bovine serum albumin (BSA) (Sigma), the tissues were immunohistochemically stained with monoclonal rabbit anti-Ki67 and anti-CC3 antibody. After incubation with primary antibody, the tissues were sequentially incubated with secondary biotin-labeled antibody and streptavidin-horseradish peroxidase. Following development with 3,3′-diaminobenzidine (DAB) liquid, the tissues were counterstained with hematoxylin.

TUNEL Staining

The tumor sections were stained using an *In Situ* Cell Death Detection Kit, POD assay (Roche), according to the manufacturer's directions for apoptosis analysis.

Enzyme-Linked Immunosorbent Assay (ELISA)

The concentrations of tumor necrosis factor α (TNF-α), IL-4, IL-10, and IFN-γ in tumor tissues and serum were determined with the use of specific mouse ELISA kits (BioLegend), according to the manufacturer's instructions.

Biochemical Analysis

ALT, AST, and urea in serum of euthanized mice were detected using an e702 Automatic Biochemical Analyzer (Roche, Germany), according to the manufacturer's instructions.

Statistical Analysis

All analyses were performed with the use of GraphPad Prism 5 statistical software (La Jolla, CA, USA). The details of the statistical tests are indicated in the respective figure legends. A two-way Student's t test was used to compare the difference between groups, where the data were approximately normally distributed. Two-way ANOVA with Tukey's multiple comparisons test was used for tumor growth curves analysis. A log-rank (Mantel-Cox) test was used for Kaplan–Meier survival experiments. For all experiments, difference with $p < 0.05$ was considered significant.

SUPPLEMENTAL INFORMATION

Supplemental Information can be found online at https://doi.org/10.1016/j.omto.2020.06.015.

AUTHOR CONTRIBUTIONS

H.Z., T.Z., R.F., Y.Y., and X.Z. planned the experiments. H.Z., T.Z., Y.P., and S.L. performed the experiments. H.Z., T.Z., P.J., W.X., H.W., and X.Z. analyzed the data. H.Z., Z.S., and X.Z. wrote the paper.

CONFLICTS OF INTEREST

The authors declare no competing interests.

ACKNOWLEDGMENTS

This study was supported by National Natural Science Foundation grants of China (grant numbers 81701572 and 81772153).

REFERENCES

1. Harbeck, N., and Gnant, M. (2017). Breast cancer. Lancet *389*, 1134–1150.
2. Torre, L.A., Bray, F., Siegel, R.L., Ferlay, J., Lortet-Tieulent, J., and Jemal, A. (2015). Global cancer statistics, 2012. CA Cancer J. Clin. *65*, 87–108.
3. Chen, W., Zheng, R., Baade, P.D., Zhang, S., Zeng, H., Bray, F., Jemal, A., Yu, X.Q., and He, J. (2016). Cancer statistics in China, 2015. CA Cancer J. Clin. *66*, 115–132.
4. Huang, J., Li, H., and Ren, G. (2015). Epithelial-mesenchymal transition and drug resistance in breast cancer (Review). Int. J. Oncol. *47*, 840–848.
5. Tang, Y., Wang, Y., Kiani, M.F., and Wang, B. (2016). Classification, Treatment Strategy, and Associated Drug Resistance in Breast Cancer. Clin. Breast Cancer *16*, 335–343.
6. The, L.; The Lancet (2018). Cancer drugs in China: affordability and creativity. Lancet *391*, 1866.
7. Granier, C., Karaki, S., Roussel, H., Badoual, C., Tran, T., Anson, M., Fabre, E., Oudard, S., and Tartour, E. (2016). [Cancer immunotherapy: Rational and recent breakthroughs]. Rev. Med. Interne *37*, 694–700.
8. Hassan, R., Alewine, C., and Pastan, I. (2016). New Life for Immunotoxin Cancer Therapy. Clin. Cancer Res. *22*, 1055–1058.
9. Shen, W., Patnaik, M.M., Ruiz, A., Russell, S.J., and Peng, K.W. (2016). Immunovirotherapy with vesicular stomatitis virus and PD-L1 blockade enhances therapeutic outcome in murine acute myeloid leukemia. Blood *127*, 1449–1458.
10. Alvey, C.M., Spinler, K.R., Irianto, J., Pfeifer, C.R., Hayes, B., Xia, Y., Cho, S., Dingal, P.C.P.D., Hsu, J., Smith, L., et al. (2017). SIRPA-Inhibited, Marrow-Derived Macrophages Engorge, Accumulate, and Differentiate in Antibody-Targeted Regression of Solid Tumors. Curr. Biol. *27*, 2065–2077.e6.
11. Gholamin, S., Mitra, S.S., Feroze, A.H., Liu, J., Kahn, S.A., Zhang, M., Esparza, R., Richard, C., Ramaswamy, V., Remke, M., et al. (2017). Disrupting the CD47-SIRPα anti-phagocytic axis by a humanized anti-CD47 antibody is an efficacious treatment for malignant pediatric brain tumors. Sci. Transl. Med. *9*, eaaf2968.
12. Melero, I., Navarro, B., Teijeira, A., and Coukos, G. (2017). Cancer immunotherapy full speed ahead. Ann. Oncol. *28* (*Suppl 12*), xii1–xii2.
13. Diken, M., Chu, K.K., and Brodsky, A.N. (2018). Translating Science into Survival: Report on the Third International Cancer Immunotherapy Conference. Cancer Immunol. Res. *6*, 10–13.
14. Lee, J.B., Chen, B., Vasic, D., Law, A.D., and Zhang, L. (2019). Cellular immunotherapy for acute myeloid leukemia: How specific should it be? Blood Rev. *35*, 18–31.
15. Haslam, A., and Prasad, V. (2019). Estimation of the Percentage of US Patients With Cancer Who Are Eligible for and Respond to Checkpoint Inhibitor Immunotherapy Drugs. JAMA Netw. Open *2*, e192535.
16. Tanoue, T., Morita, S., Plichta, D.R., Skelly, A.N., Suda, W., Sugiura, Y., Narushima, S., Vlamakis, H., Motoo, I., Sugita, K., et al. (2019). A defined commensal consortium elicits CD8 T cells and anti-cancer immunity. Nature *565*, 600–605.
17. Skelly, A.N., Sato, Y., Kearney, S., and Honda, K. (2019). Mining the microbiota for microbial and metabolite-based immunotherapies. Nat. Rev. Immunol. *19*, 305–323.
18. Helmink, B.A., Khan, M.A.W., Hermann, A., Gopalakrishnan, V., and Wargo, J.A. (2019). The microbiome, cancer, and cancer therapy. Nat. Med. *25*, 377–388.
19. Zeng, Q., and Jewell, C.M. (2019). Directing toll-like receptor signaling in macrophages to enhance tumor immunotherapy. Curr. Opin. Biotechnol. *60*, 138–145.
20. Chowdhury, S., Castro, S., Coker, C., Hinchliffe, T.E., Arpaia, N., and Danino, T. (2019). Programmable bacteria induce durable tumor regression and systemic antitumor immunity. Nat. Med. *25*, 1057–1063.
21. Gopalakrishnan, V., Helmink, B.A., Spencer, C.N., Reuben, A., and Wargo, J.A. (2018). The Influence of the Gut Microbiome on Cancer, Immunity, and Cancer Immunotherapy. Cancer Cell *33*, 570–580.
22. Zitvogel, L., Daillère, R., Roberti, M.P., Routy, B., and Kroemer, G. (2017). Anticancer effects of the microbiome and its products. Nat. Rev. Microbiol. *15*, 465–478.
23. Roy, S., and Trinchieri, G. (2017). Microbiota: a key orchestrator of cancer therapy. Nat. Rev. Cancer *17*, 271–285.
24. Zitvogel, L., Ayyoub, M., Routy, B., and Kroemer, G. (2016). Microbiome and Anticancer Immunosurveillance. Cell *165*, 276–287.
25. Feng, Y., Mu, R., Wang, Z., Xing, P., Zhang, J., Dong, L., and Wang, C. (2019). A toll-like receptor agonist mimicking microbial signal to generate tumor-suppressive macrophages. Nat. Commun. *10*, 2272.
26. Kirkham, L.A., Kerr, A.R., Douce, G.R., Paterson, G.K., Dilts, D.A., Liu, D.F., and Mitchell, T.J. (2006). Construction and immunological characterization of a novel nontoxic protective pneumolysin mutant for use in future pneumococcal vaccines. Infect. Immun. *74*, 586–593.
27. Liu, Y., Wang, H., Zhang, S., Zeng, L., Xu, X., Wu, K., Wang, W., Yin, N., Song, Z., Zhang, X., and Yin, Y. (2014). Mucosal immunization with recombinant fusion protein DnaJ-ΔA146Ply enhances cross-protective immunity against Streptococcus pneumoniae infection in mice via interleukin 17A. Infect. Immun. *82*, 1666–1675.
28. Su, Y., Li, D., Xing, Y., Wang, H., Wang, J., Yuan, J., Wang, X., Cui, F., Yin, Y., and Zhang, X. (2017). Subcutaneous Immunization with Fusion Protein DnaJ-ΔA146Ply without Additional Adjuvants Induces both Humoral and Cellular Immunity against Pneumococcal Infection Partially Depending on TLR4. Front. Immunol. *8*, 686.
29. Wu, J., Wu, K., Xu, W., Yuan, T., Wang, X., Zhang, J., Min, Y., Yin, Y., and Zhang, X. (2018). Engineering detoxified pneumococcal pneumolysin derivative ΔA146PLY for self-biomineralization of calcium phosphate: Assessment of their protective efficacy in murine infection models. Biomaterials *155*, 152–164.
30. Fu, R., Deng, Q., Zhang, H., Hu, X., Li, Y., Liu, Y., Hu, J., Luo, Q., Zhang, Y., Jiang, X., et al. (2018). A novel autophagy inhibitor berbamine blocks SNARE-mediated autophagosome-lysosome fusion through upregulation of BNIP3. Cell Death Dis. *9*, 243.
31. Zheng, Y., Gu, S., Li, X., Tan, J., Liu, S., Jiang, Y., Zhang, C., Gao, L., and Yang, H.T. (2017). Berbamine postconditioning protects the heart from ischemia/reperfusion injury through modulation of autophagy. Cell Death Dis. *8*, e2577.
32. Wang, S., Liu, Q., Zhang, Y., Liu, K., Yu, P., Liu, K., Luan, J., Duan, H., Lu, Z., Wang, F., et al. (2009). Suppression of growth, migration and invasion of highly-metastatic human breast cancer cells by berbamine and its molecular mechanisms of action. Mol. Cancer *8*, 81.
33. Zhang, Y., Cao, Y., Sun, X., Feng, Y., Du, Y., Liu, F., Yu, C., and Jin, F. (2017). Chloroquine (CQ) exerts anti-breast cancer through modulating microenvironment and inducing apoptosis. Int. Immunopharmacol. *42*, 100–107.
34. Bianchini, G., Balko, J.M., Mayer, I.A., Sanders, M.E., and Gianni, L. (2016). Triple-negative breast cancer: challenges and opportunities of a heterogeneous disease. Nat. Rev. Clin. Oncol. *13*, 674–690.
35. Nauts, H.C., Swift, W.E., and Coley, B.L. (1946). The treatment of malignant tumors by bacterial toxins as developed by the late William B. Coley, M.D., reviewed in the light of modern research. Cancer Res. *6*, 205–216.
36. Kiselyov, A., Bunimovich-Mendrazitsky, S., and Startsev, V. (2015). Treatment of non-muscle invasive bladder cancer with Bacillus Calmette-Guerin (BCG): Biological markers and simulation studies. BBA Clin. *4*, 27–34.
37. Greig, S.L. (2015). Brexpiprazole: First Global Approval. Drugs *75*, 1687–1697.
38. Esener, O., Balkan, B.M., Armutak, E.I., Uvez, A., Yildiz, G., Hafizoglu, M., Yilmazer, N., and Gurel-Gurevin, E. (2018). Donkey milk kefir induces apoptosis and suppresses proliferation of Ehrlich ascites carcinoma by decreasing iNOS in mice. Biotech. Histochem. *93*, 424–431.
39. Zhao, W., Zhang, X., Zhou, Z., Sun, B., Gu, W., Liu, J., and Zhang, H. (2018). Liraglutide inhibits the proliferation and promotes the apoptosis of MCF-7 human breast cancer cells through downregulation of microRNA-27a expression. Mol. Med. Rep. *17*, 5202–5212.
40. Wang, Y., Dai, Y.X., Wang, S.Q., Qiu, M.K., Quan, Z.W., Liu, Y.B., and Ou, J.M. (2018). miR-199a-5p inhibits proliferation and induces apoptosis in hemangioma

cells through targeting HIF1A. Int. J. Immunopathol. Pharmacol. *31*, 394632017749357.

41. Rahmani, M., Nkwocha, J., Hawkins, E., Pei, X., Parker, R.E., Kmieciak, M., Leverson, J.D., Sampath, D., Ferreira-Gonzalez, A., and Grant, S. (2018). Cotargeting BCL-2 and PI3K Induces BAX-Dependent Mitochondrial Apoptosis in AML Cells. Cancer Res. *78*, 3075–3086.

42. Karki, R., Man, S.M., and Kanneganti, T.D. (2017). Inflammasomes and Cancer. Cancer Immunol. Res. *5*, 94–99.

43. Hu, Q., Zhao, F., Guo, F., Wang, C., and Fu, Z. (2017). Polymeric Nanoparticles Induce NLRP3 Inflammasome Activation and Promote Breast Cancer Metastasis. Macromol. Biosci. *17*, 1700273.

44. Ershaid, N., Sharon, Y., Doron, H., Raz, Y., Shani, O., Cohen, N., Monteran, L., Leider-Trejo, L., Ben-Shmuel, A., Yassin, M., et al. (2019). NLRP3 inflammasome in fibroblasts links tissue damage with inflammation in breast cancer progression and metastasis. Nat. Commun. *10*, 4375.

45. Weichand, B., Popp, R., Dziumbla, S., Mora, J., Strack, E., Elwakeel, E., Frank, A.-C., Scholich, K., Pierre, S., Syed, S.N., et al. (2017). S1PR1 on tumor-associated macrophages promotes lymphangiogenesis and metastasis via NLRP3/IL-1β. J. Exp. Med. *214*, 2695–2713.

46. Littmann, M., Albiger, B., Frentzen, A., Normark, S., Henriques-Normark, B., and Plant, L. (2009). Streptococcus pneumoniae evades human dendritic cell surveillance by pneumolysin expression. EMBO Mol. Med. *1*, 211–222.

47. Zhang, H., Jiao, Y., Shi, C., Song, X., Chang, Y., Ren, Y., and Shi, X. (2018). Berbamine suppresses cell viability and induces apoptosis in colorectal cancer via activating p53-dependent apoptotic signaling pathway. Cytotechnology *70*, 321–329.

48. Zhang, H., Jiao, Y., Shi, C., Song, X., Chang, Y., Ren, Y., and Shi, X. (2018). Berbamine suppresses cell proliferation and promotes apoptosis in ovarian cancer partially via the inhibition of Wnt/β-catenin signaling. Acta Biochim. Biophys. Sin. (Shanghai) *50*, 532–539.

49. Zhao, Y., Lv, J.J., Chen, J., Jin, X.B., Wang, M.W., Su, Z.H., Wang, L.Y., and Zhang, H.Y. (2016). Berbamine inhibited the growth of prostate cancer cells in vivo and in vitro via triggering intrinsic pathway of apoptosis. Prostate Cancer Prostatic Dis. *19*, 358–366.

50. Wang, G.Y., Lv, Q.H., Dong, Q., Xu, R.Z., and Dong, Q.H. (2009). Berbamine induces Fas-mediated apoptosis in human hepatocellular carcinoma HepG2 cells and inhibits its tumor growth in nude mice. J. Asian Nat. Prod. Res. *11*, 219–228.

51. Wei, Y.L., Xu, L., Liang, Y., Xu, X.H., and Zhao, X.Y. (2009). Berbamine exhibits potent antitumor effects on imatinib-resistant CML cells in vitro and in vivo. Acta Pharmacol. Sin. *30*, 451–457.

52. Handgretinger, R., and Schilbach, K. (2018). The potential role of γδ T cells after allogeneic HCT for leukemia. Blood *131*, 1063–1072.

53. Silva-Santos, B., Serre, K., and Norell, H. (2015). γδ T cells in cancer. Nat. Rev. Immunol. *15*, 683–691.

54. Zou, C., Zhao, P., Xiao, Z., Han, X., Fu, F., and Fu, L. (2017). γδ T cells in cancer immunotherapy. Oncotarget *8*, 8900–8909.

55. Silva-Santos, B., Mensurado, S., and Coffelt, S.B. (2019). γδT cells: pleiotropic immune effectors with therapeutic potential in cancer. Nat. Rev. Cancer *19*, 392–404.

56. Hodgins, N.O., Wang, J.T., and Al-Jamal, K.T. (2017). Nano-technology based carriers for nitrogen-containing bisphosphonates delivery as sensitisers of γδ T cells for anticancer immunotherapy. Adv. Drug Deliv. Rev. *114*, 143–160.

57. Havran, W.L. (2018). Specialized Antitumor Functions for Skin γδ T Cells. J. Immunol. *200*, 3029–3030.

58. Tanaka, Y., Morita, C.T., Tanaka, Y., Nieves, E., Brenner, M.B., and Bloom, B.R. (1995). Natural and synthetic non-peptide antigens recognized by human gamma delta T cells. Nature *375*, 155–158.

59. Agarwal, V., Kuchipudi, A., Fulde, M., Riesbeck, K., Bergmann, S., and Blom, A.M. (2013). Streptococcus pneumoniae endopeptidase O (PepO) is a multifunctional plasminogen- and fibronectin-binding protein, facilitating evasion of innate immunity and invasion of host cells. J. Biol. Chem. *288*, 6849–6863.